Check for updates

A Journal of the Gesellschaft Deutscher Chemiker

Angewandte International Edition Chemie

GDCh

www.angewandte.org

Accepted Article

Title: Ultrathin Two-dimentional Layered Composite Carbosilicates from in situ Unzipped Carbon Nanotubes and Exfoliated Bulk Silica

Authors: Yuxiao Ding, Yumeng Liu, Alexander Yu. Klyushin, Liyun Zhang, Gengxu Han, Zigeng Liu, Jianying Li, Bingsen Zhang, Kang Gao, Wei Li, Rüdiger-A Eichel, Xiaoyan Sun, Zhen-An Qiao, and Saskia Heumann

This manuscript has been accepted after peer review and appears as an Accepted Article online prior to editing, proofing, and formal publication of the final Version of Record (VoR). The VoR will be published online in Early View as soon as possible and may be different to this Accepted Article as a result of editing. Readers should obtain the VoR from the journal website shown below when it is published to ensure accuracy of information. The authors are responsible for the content of this Accepted Article.

To be cited as: *Angew. Chem. Int. Ed.* **2023**, e202318043

Link to VoR: https://doi.org/10.1002/anie.202318043

WILEY VCH

10.1002/anie.202318043

15213773, ja, Downloaded from https://onlinelibrary.wiley.com/doi/10.1002/anie.202318043 by Fritz-Haber-Institut Der Max-Planck-Gesellschaft, Wiley Online Library on [09/01/2024]. See the Terms and Conditions (https://onlinelibrary.wiley.com/terms-and-conditions) on Wiley Online Library for rules of use; OA articles are governed by the applicable Creative Commons License

WILEY VCH

RESEARCH ARTICLE

Ultrathin Two-dimensional Layered Composite Carbosilicates from in situ Unzipped Carbon Nanotubes and Exfoliated Bulk Silica

Yuxiao Ding,[a,c] Yumeng Liu,[b] Alexander Yu. Klyushin,[d,e] Liyun Zhang,[f] Gengxu Han,[b] Zigeng Liu,[c,g] Jianying Li,[h] Bingsen Zhang,[f] Kang Gao,[a] Wei Li,[i] Rüdiger-A Eichel,[g] Xiaoyan Sun,[h]* Zhen-An Qiao,[b]* and Saskia Heumann[c]

[a] Prof. Dr. Y. Ding, Dr. K. Gao
Lanzhou Institute of Chemical Physics, Chinese Academy of Sciences, Tianshui Middle Road 18, 730000 Lanzhou, China

[b] Y. Liu, G. Han, Prof. Dr. Z. A. Qiao
State Key Laboratory of Inorganic Synthesis and Preparative Chemistry, Jilin University, Qianjin Street 2699, 130012 Changchun, China
E-mail: qiaozhenan@jlu.edu.cn

[c] Prof. Dr. Y. Ding, Dr. Z. Liu, Dr. S. Heumann
Max Planck Institute for Chemical Energy Conversion, Stiftstrasse 34-36, Mülheim an der Ruhr, Germany

[d] Dr. A. Klyushin
Fritz Haber Institute of the Max Planck Society, Faradayweg 4-6, 14195 Berlin, Germany

[e] Dr. A. Klyushin
Research Group Catalysis for Energy, Helmholtz-Zentrum Berlin für Materialien und Energie GmbH, Albert-Einstein-Strasse 15, 12489 Berlin, Germany

[f] L. Zhang, B. Zhang
Institute of Metal Research, Chinese Academy of Sciences, Wenhua Road 72, 110016 Shenyang, China

[g] Dr. Z. Liu, Prof. Dr. R. Eichel
Institut für Energie und Klimaforschung (IEK-9), Forschungszentrum Jülich GmbH, Leo-Brandt-Str., 52425 Jülich, Germany

[h] Dr. J. Li, Prof. Dr. X. Sun
Qingdao Institute of Bioenergy and Bioprocess Technology, Chinese Academy of Sciences, Songling Road 189, Laoshan District, 266101 Qingdao, China
E-mail: sunxy@qibebt.ac.cn

[i] Prof. Dr. W. Li
Laboratory of Advanced Materials Department of Chemistry, Fudan University, Songhu 2205, 200433 Shanghai, China

Supporting information for this article is given via a link at the end of the document.

This article is protected by copyright. All rights reserved.

10.1002/anie.202318043

RESEARCH ARTICLE

A key task in today's inorganic synthetic chemistry is to develop effective reactions, routes, and associated techniques aiming to create new functional materials with specifically desired multilevel structures and properties. Herein, we report an ultrathin two-dimensional layered composite of graphene ribbon and silicate via a simple and scalable one-pot reaction, which leads to the creation of a novel carbon-metal-silicate hybrid family: carbosilicate. The graphene ribbon is in-situ formed by unzipping carbon nanotubes, while the ultrathin silicate is in-situ obtained from bulk silica or commercial glass; transition metals (Fe or Ni) oxidized by water act as bridging agent, covalently bonding the two structures. The unprecedented structure combines the superior properties of the silicate and the nanocarbon, which triggers some specific novel properties. All processes during synthesis are complementary to each other. The associated synergistic chemistry could stimulate the discovery of a large class of more interesting, functionalized structures and materials.

Introduction

With the vibrant growth of emerging sciences and the rapid development of new technologies, there is greater demand for chemists to create more multi-phase inorganic materials with specific structures and functions.[1] Conventional materials including glass, ceramics, and metals have been widely investigated and refined for composites applications, where carbon has proven to be the most successful reinforcement and a matrix for these compositions.[2] The challenging parts are the complexity as well as our limited understanding of hybridizing processes in both theoretical and experimental executions.[1] Therefore, working on the development of novel and effective synthetic technologies and carrying out related theoretical studies is of high significance for the scalable creation of a large class of new matters.

Generally, two-dimensional (2D) materials are expected to have better mechanical and chemical response than their bulk form due to confinement of electrons and the absence of weak interlayer interactions.[3] Ultrathin 2D structures like graphene nanoribbon and silicate have attracted increasing attention owing to their unique physical and chemical features.[4] According to the edge patterns, graphene nanoribbons[5] have versatile electronic properties, therefore are excellent candidates for application in electronic devices.[6] Layered silicates have been widely used as catalyst supports as well as adsorber.[7] They also have good performance in applications that involve charge transfer processes, including sensors, field emission devices, and photocatalytic applications.[8] Considering their superior independent properties, the hybridization of the graphene ribbon and the layered silicate is of great interest to adjust their intrinsic properties and achieve properties which are absent in pure materials. However, chemically bonding of carbon and silicate generally cannot happen due to their surface inertness to each other. Herein, we report a novel and effective synthetic route to fulfill the covalent bonding of the two structures leading to the creation of a large family of the carbon and silicate composite: carbosilicate.

Results and Discussion

In a typical synthesis process, three commercially available agents: carbon nanotubes (CNT), silica and metallic iron powder are mixed in an autoclave with deionized water, following one simple hydrothermal treatment (experimental details in SI, Supplementary Information). The obtained product is collected via filtration and washed with ammonia to remove the unreacted silica. Figure 1 shows a schematic drawing of the potential "unzipping and zipping" process during synthesis. Generally, an "unzipping" process from CNT into graphene nanoribbons takes place, while the bulk silica is "unzipped" and reforms into layered silicate. The reaction between iron and water ($2Fe^0 + 6H_2O \rightarrow 2Fe^{3+} + 6OH^- + 3H_2$), is most likely the "scissor" for the two unzipping processes and the formed iron cations "zip" the silicate and graphene nanoribbon giving an ultrathin carbosilicate. Predictably, other transition metals such as nickel and cobalt can also work for the unzipping processes like iron. It is worth to note that the "unzipping" process of the CNT enhances the formation of the layered silicate, without which the commercial glass cannot form any layered silicate. Meanwhile, the "unzipping" process of the silica is indispensable for the CNT unzipping process, without which the CNT remains the tube structure (Figure S1). The two "unzipping" processes in return boost the reaction between iron and water (as the main driving force for the "scissor"), continuously extracting the only but useful byproduct hydrogen from water. In sum, all these reactions are interdependent and promote each other, making the impossible possible. The synergistic effect of the "impossible" reactions also sheds a light to develop novel reactions and structures by combining some unusual processes.

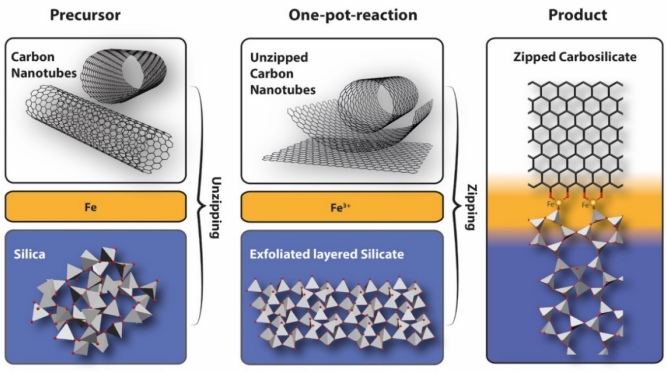

Figure 1. Schematic illustration of the potential "unzipping and zipping" synthesis process of the carbosilicate. The image is not drawn to scale and only one simple possible stacking form of the product is provided for visualization.

As linking agent, iron has significant influence on the products. When the added iron content is 2.5 wt% of the carbon, the CNT (Figure 2a, S2) only partially open forming a mixture of layered carbosilicate and unopened CNT (Figure S3). By adding excessive amount of iron (65 wt% of carbon), most CNT are unzipped with the formation of the carbosilicate, in which up to 10 wt% iron content can be achieved (10Fe-CSiO$_x$). The sample exhibits mainly layered structures as demonstrated by scanning electron microscopy (SEM, Figure 2b). The transmission electron

This article is protected by copyright. All rights reserved.

15213773, ja, Downloaded from https://onlinelibrary.wiley.com/doi/10.1002/anie.202318043 by Fritz-Haber-Institut Der Max-Planck-Gesellschaft, Wiley Online Library on [09/01/2024]. See the Terms and Conditions (https://onlinelibrary.wiley.com/terms-and-conditions) on Wiley Online Library for rules of use; OA articles are governed by the applicable Creative Commons License

10.1002/anie.202318043

microscopy (TEM) further confirms the 2D structures with 3-4 nm thickness (Figures 2c, d). Mapping information (Figures 2e-i) verifies the formation of associated layered carbon and iron-involved silicate (we name this as iron silicate), wherein the silicate adheres to the carbon surface. The iron as bridging agent for the two phases, also scaffold the 2D structure. When the iron is removed with sulfuric acid, the structure collapses, and agglomerates into big chunks (Figure S4). Although CNT are mostly unzipped (Figure S5), there are still trace tube residue observable. In a formed fine ultrathin 2D structure, the atomic ratio of Fe, C, Si, O can be confirmed as 3: 4: 5: 21 (Figure S6). Nevertheless, the carbon and silicate phases are independent of each other, allowing the ratio to be adjusted in a very wide range.

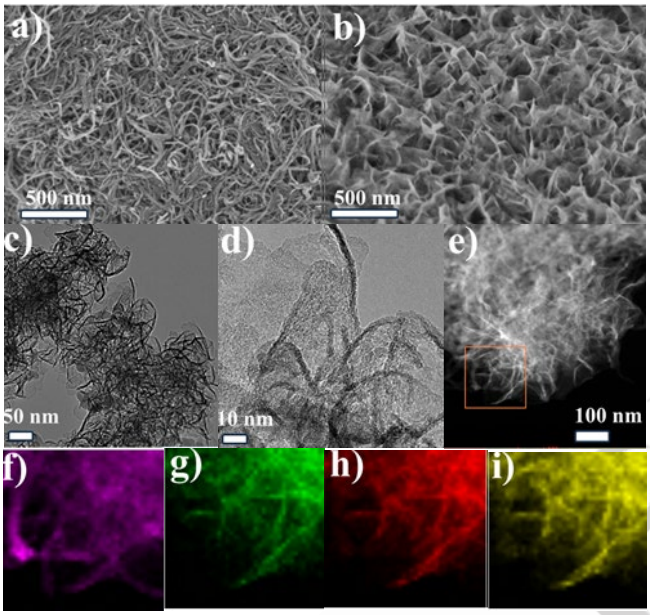

Figure 2. a) SEM images of the CNT. b) SEM images of 10Fe-CSiO$_x$ (share same scale bar with a). TEM images of the 10Fe-CSiO$_x$ in low c) and high d) resolution e) STEM images of the sample (mapping information are taken within the orange box). Element mapping images of the nanocomposites f) C, g) Fe, h) O and i) Si.

Basically, carbon surfaces are covered by different oxygen functional groups which can adsorb or react with metal species (Figure S7). The functional groups on CNT result in the adsorption of 0.62 wt% of iron (FeCNT, Table S1). The adsorbed metal species have the ability, through the energy input, to unzip CNT by sequential carbon-carbon bond cleavage.[9] The unzipped carbon edges can be terminated by forming phenol groups which can further saturate with iron species. Meanwhile, the formed layered silicate has abundant hydroxyl groups on the surface, which can also be terminated by iron species.[10] Thus, by stabilizing both structures, iron ions combine them to form the carbosilicate. When CNT was replaced with a fully functionalized spherical shaped non-graphitic carbon, a homogeneous adsorption of the iron silicate on the carbon surface can also be observed (Figure S8); while with a non-defective tube carbon (annealed at 3000ºC to remove defects), no composites can be formed (Figure S9). Therefore, the functionality on carbon surface is indispensable for the formation of the composite. This is proved in the following parts.

The formed graphene ribbons have maintained the sp^2 hybridized structures from CNT. Figure 3a shows the near-edge X-ray adsorption fine structures (NEXAFS) C k-edge spectra of different samples, confirming the preservation of the sp^2 structures after the unzipping process. X-ray diffraction (XRD) curves suggest that the graphitic structures are maintained for different samples (Figure S10). A change of the C k-edge signal intensity in the region attributed to C-O species on the CNT surface can be observed in comparison to the carbosilicate samples, demonstrating a blocking effect of the surface functionality by the silicate. For further investigations of the surface functional groups and their interaction with silicate, a stepwise thermal analysis[11] is performed. The original CNT has specific functional groups on the surface, which thermally decomposed one by one under the release of CO_2 (m/z signal 44) or CO (m/z signal 28) at certain temperatures (Figures S11, 12). Figure 3b and Figure S13 show the mass spectra and the derived quantities of the functional groups on different carbon surface. For CNT, it contains various functional groups (six steps are used to distinguish them). For the FeCNT, as iron ions reacted with oxygen functional groups, the relative desorption of the oxygen functionality happens mainly at one specific temperature around 800ºC. This is because most of the functional groups on the CNT surface are stabilized by forming Fe-O-C bonds. For the 10Fe-CSiO$_x$ sample, the formation of the C-O-Fe (silicate) shows even better stabilizing effect on the C-O bond and the relative desorption temperature can reach to 1000°C. This is direct evidence of the oxygen functional groups reacting with the iron silicate. Although the C k-edge spectrum and the NEXAFS spectrum shows only small amounts of oxygen on the surface of the formed carbosilicate, a clear increase of the oxygen content on the carbon surface could be confirmed by ^{13}C NMR (Figure 3c). The CNT displays a broad ^{13}C peak at 139 ppm, which is ascribed to the sp^2 carbon from the carbon backbone, while the oxidized carbon on the surface displays a shoulder peak at around 235 ppm. The intensity ratio of the oxidized/bulk part increases from 0.26 of CNT to 0.46 of 2.1Fe-CSiO$_x$, and 0.57 of 10Fe-CSiO$_x$, respectively. It is explainable, as the unzipping process must introduce more oxidized carbon edges.

The NEXAFS of iron L-edges (Figure 3d) of different samples confirm the presence of oxidized iron in the composites (mainly as octahedral form). The Si-L and Si-K edges in the electron energy loss spectra (EELS) of the carbosilicate stay at the similar position in comparison to the SiO_2 references (Figures S14-S15), demonstrating that the bulk silica is not reduced. The observed vibration of Si-O-Si bond at 1006 cm^{-1} in the IR spectra supports the formation of the new bond (Figure 3e).[12] The blue shift of 26 cm^{-1} for the Si-O-Si peak in comparison to iron silicate (1032 cm^{-1})[13] is most likely caused by the interaction with carbon. The unzipping process of CNT is also supported by the Raman spectra in Figure S16. The G bands of the carbosilicate shift to lower wavenumbers in comparison to the CNT, which is a typical shift from a curved graphitic structure to a plain structure.[14]

This article is protected by copyright. All rights reserved.

15213773, ja, Downloaded from https://onlinelibrary.wiley.com/doi/10.1002/anie.202318043 by Fritz-Haber-Institut Der Max-Planck-Gesellschaft, Wiley Online Library on [09/01/2024]. See the Terms and Conditions (https://onlinelibrary.wiley.com/terms-and-conditions) on Wiley Online Library for rules of use; OA articles are governed by the applicable Creative Commons License

Accepted Manuscript

10.1002/anie.202318043

RESEARCH ARTICLE

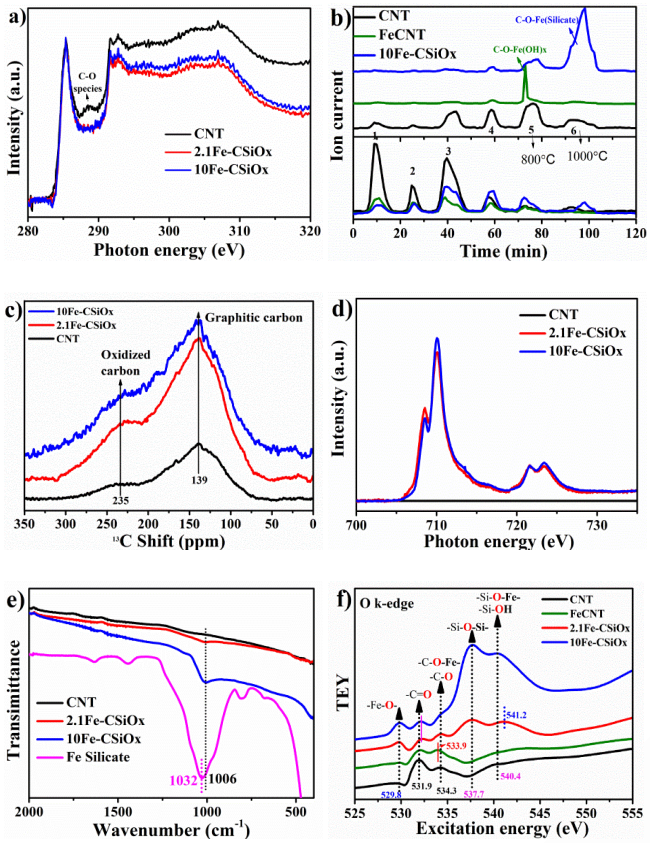

Figure 3. a) NEXAFS C k-edge of the CNT and the carbosilicates. b) Quantified carbon oxides content of the different samples via mass spectra when heating them at different temperatures. The m/z 44 signal is attributed to CO^{2+}. FeCNT is the iron chemically adsorbed on CNT. The m/z 28 signal is attributed to CO^{+}. The programmed temperatures (detail procedure in Figure S11) are used for removing different functional groups on carbon surface. The six steps with six peaks represent: 1) 253°C carboxylic, 2) 315°C, lactone (on zigzag edges) 3) 510°C anhydride, 4) 620°C ethers, 5) 800°C phenol and 6) 1000°C carbonyl groups, respectively. c) NMR spectra of different samples. The intensity ratios of the oxygen functionalized carbon at 235 ppm and the intensity of the main carbon peak at 139 ppm are 0.57, 0.46 and 0.26 for 10Fe-CSiO$_x$, 2.1Fe-CSiO$_x$ and CNT, respectively. d) NEXAFS spectra of the Fe L-edge of different samples. e) ATR-IR spectra of different samples. f) NEXAFS spectra of the O K-edge of different samples.

In the formed carbosilicate, oxygen is the connecting agent for all other elements. Figure 3f shows the NEXAFS O k-edge of different samples. The peaks of CNT can be assigned to C=O (531.9 eV) and C-O (534.3 eV). For the FeCNT, the formation of C-O-Fe leads to an increase of intensity for the C-O bond and the peak position of the single bond shifts from 534.3 eV to 533.9 eV. For the carbosilicate samples, the peak intensities of the C-O single bond are also enhanced and the newly formed peaks at 529.8 eV are attributed to Fe-O-C.[15] The peak of the C-O bond almost merges with the Si-O-Si peak in the case of 10Fe-CSiO$_x$, which suggests the reaction between the carbon surface functionality and the silicates. The two peaks at 537.7 eV and 540.1 eV derived from Si-O bond also change with the increase of the iron concentration, indicating the influence from the connection (iron) with the carbon phase. The X-ray photoelectron spectroscopy (XPS) data of different elements support the above conclusions, and the details can be seen in Figures S17 to S20.

Based on above results, the proposed structure of the composites in Figure 1 can be confirmed. In this part, the formation mechanism of the carbosilicate is discussed in detail. The synergistic chemistry can be partly revealed by checking the products during the synthesis. Figure S21 shows the iron content in the solution tested by inductively coupled plasma optical emission spectrometer (ICP-OES). The iron content displays a continuously increasing trend, reaching up to 16 ppm after 24 hours reaction, while pure iron and water show no detectable products at the same condition. The unzipping process of the CNT is a redox process from C(0) to C(oxides), while Fe^{3+} is considered as the main unzipping agent. This can be verified by the theoretical calculation in Figure 4a, where the open energy of the first carbon-carbon bond without iron involvement (3.3 eV) is five times higher than the energy with iron involved (0.06 eV). Considering the effect of oxygen functionality, the equation could be $C_x - OH + OH^- + Fe^{3+} \rightarrow (C_x - OFe)^+ + H_2O$. The Mössbauer spectrum of the pure iron silicate in Figure 4b indicates almost 100% Fe^{3+}, while the 10Fe-CSiO$_x$ has around 85% Fe^{3+} and 15% Fe^{2+}. Considering the abundant oxygen functionality on the carbon surface, the layered silicates are supposed to be linked on it (Figure 4d). After breaking the first carbon-carbon bond of the CNT, the following unzipping process is much easier (Figure 4d). Additionally, the functional groups on the carbon surface are also confirmed to be favorable for the unzipping process (Figure S8, S9), and the exposed carbon open edge need to be stabilized by consuming OH^- and iron ions to form a positive carbon surface $(C_x\text{-O-Fe})^+$, which further bonding the silicate layer.

The OH^- is the main agent for reacting with silica. The consumption during the reaction with silica leads to a decrease of the pH (Figure 4e) although even through the reaction of iron and water, additional OH^- is produced. The consuming of the OH^- also becomes a driving force for the water-iron reaction. The "unzipping" process of silica can be described as following: the low concentration of OH^- reacts with the Si-O-Si units of the silica forming silicate ions ($SiO_2 + 2OH^- \rightarrow SiO_3^{2-} + H_2O$; $SiO_2 + 4OH^- \rightarrow SiO_4^{4-} + 2H_2O$). The consumption of silica can be observed by the shrinking process of the bulk structure during the reaction (Figure S22). The continuous increase of the silicate signal in the solutions can be confirmed via UV-Vis spectra (Figure 4f). The silicate ions resemble and condense to form the layered silicate on positive carbon surface. ($C_x - O - Fe + SiO_3^{2-} \rightarrow C_x - O - Fe - O - SiO_2^-$; $C_x - O - Fe + SiO_4^{4-} \rightarrow C_x - O - Fe - O - SiO_3^{3-}$;) The adsorption energy of the silicates on the carbon surface is much lower than that of OH^- (Figure S23). When the positive carbon surface is fully covered, an ultrathin layered silicate is also formed. In most commonly encountered silicates, each silicon atom occupies the center of an idealized tetrahedron whose corners are four oxygen atoms, while each oxygen atom is also a bridge between two silicon atoms.[16] It is worth to note, if the concentration of the OH^- is too high, the SiO_2 can be mainly dissolved to form silicate ions in the solution (Figure S24), where

This article is protected by copyright. All rights reserved.

15213773, ja, Downloaded from https://onlinelibrary.wiley.com/doi/10.1002/anie.202318043 by Fritz-Haber-Institut Der Max-Planck-Gesellschaft, Wiley Online Library on [09/01/2024]. See the Terms and Conditions (https://onlinelibrary.wiley.com/terms-and-conditions) on Wiley Online Library for rules of use; OA articles are governed by the applicable Creative Commons License

10.1002/anie.202318043

RESEARCH ARTICLE

no detectable solid silicate form. The hydrogen from water-iron reaction is detectable via a portable hydrogen detector, which is highly important as extracting hydrogen from water provides OH^-. To explore the effects of the other metals than iron on the synergistic reaction, different transition metals, like Ni, are also being used instead of iron during the synthesis. For the reaction with 2.5 mg Ni powder, the final product contains less Ni species than in the case of the iron sample. The obtained final product 0.4Ni-$CSiO_x$ has only 0.4 wt% of Ni species, which also exhibits a nice, layered structure like the iron sample (Figure S25). This indicates that different metals other than iron may also be used as the linker for getting carbosilicates with different metal species.

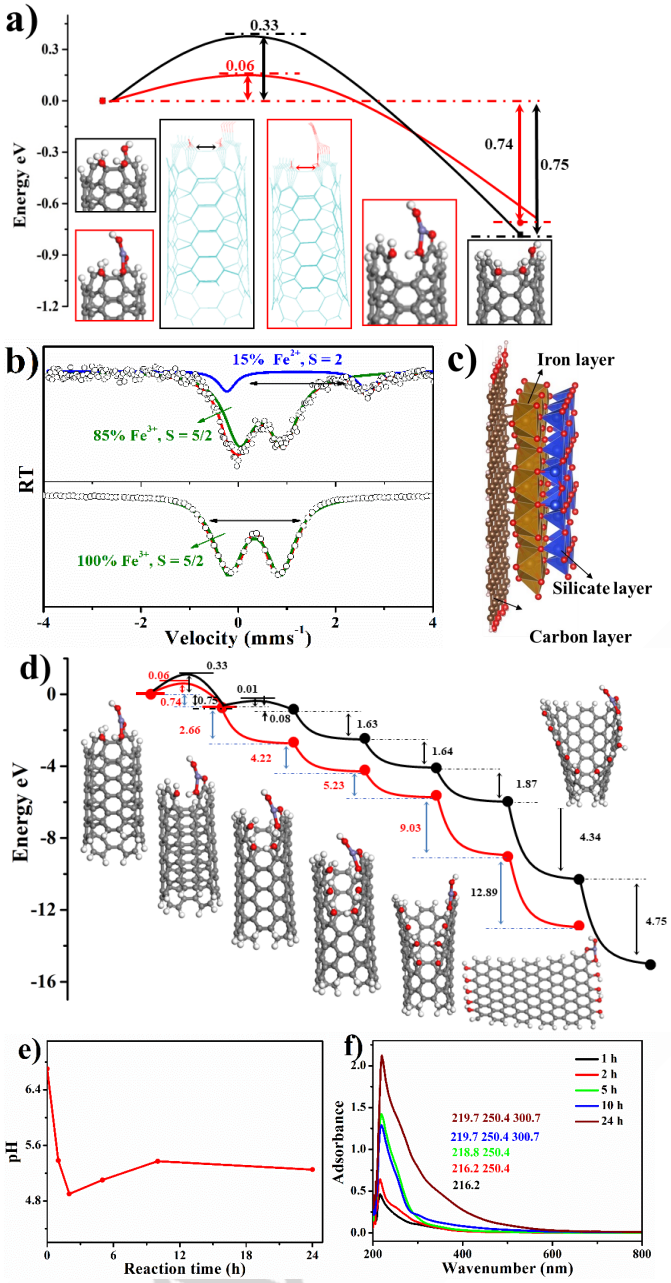

Figure 4. a) Theoretical calculation of the energy when breaking the first carbon-carbon bond of CNT. The red part is with the involvement of the iron ions and the black one is without iron. b) Mössbauer spectra of ^{57}Fe in 10Fe-$CSiO_x$ at 80 K (upper one) and the iron silicate without involvement of any carbon (lower one). The Y- axes is relative transmission (RT). c) The unzipping process of the CNT. d) The calculated model of the carbosilicate. e) The pH value of the solutions during synthesis of the 10Fe-$CSiO_x$. f) UV-Vis spectra of the synthesis solutions for different reaction time (the numbers indicate the positions of the main peak and shoulder peaks). The spectra show the characteristic peaks of silicate from 216.2 nm to 219.7 nm. The shift might be caused by bonding formation of the silicate with the decomposed carbon debris. The gradually arising shoulder peaks could be the result of the adsorption of those carbon debris.

Figure 5a shows the nitrogen adsorption-desorption curve of different samples. CNT exhibits a surface area of 232 m^2g^{-1} as determined by Brunauer-Emmet-Teller (BET) analysis.[17] The unzipping is supposed to have no significant influence on the surface area. However, with the formation of the layered composites, the surface area increased to 289 m^2g^{-1} (2.1Fe-$CSiO_x$) and 312 m^2g^{-1} (10Fe-$CSiO_x$), respectively. The hysteresis of the silicate samples can be classified as H1, which points to a narrow pore distribution of relatively uniform meso-pores. The increase of the surface area might result from the exfoliation of multi-layered carbon and the silicate. Surprisingly, with increasing the amount of iron, a mesoporous structure is formed with a fixed pore size at around 2 nm, determined by the Barrett-Joyner-Halenda (BJH) theory[18] (Figure 5b). Compared to the precursors and many other materials, the formed materials have higher surface area, more interfaces, and defects, which can be used as superior supports and adsorbents.

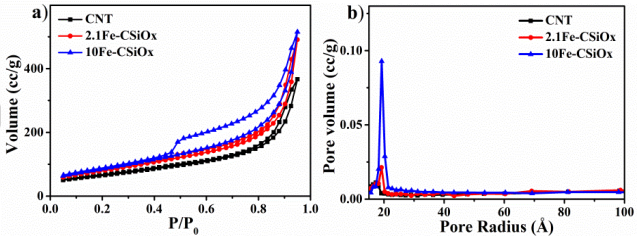

Figure 5. a) N_2 sorption measurements and b) pore size distribution of different samples.

Carbon based materials as material carrier is promising in the application of energy area.[19] In this part, we show some other potential directions of the newly formed 2D structure. The aim is not giving the most optimized performance but providing promising possibilities. Figure S26 shows the performance of different samples for water oxidation, from which the 0.4Ni-$CSiO_x$ clearly exhibits much better performance than the commercial $NiCoO_x$. Compared with one of the best commercial catalysts IrO_x, the sample also shows higher currents at higher potentials under the same conditions. This phenomenon might be caused by the better hydrophilicity of the carbosilicate than IrOx. This is supported by the stability test, in which the IrOx shows bumps in the current due to bubble accumulation (Figure S27a). This simple and basic comparison is not sufficient to state that the carbosilicate is a better water oxidation catalyst than IrO_x, but this application does demonstrate the good conductivity and hydrophilicity of the material (water angle test in Figure S27b). A

This article is protected by copyright. All rights reserved.

15213773, ja, Downloaded from https://onlinelibrary.wiley.com/doi/10.1002/anie.202318043 by Fritz-Haber-Institut Der Max-Planck-Gesellschaft, Wiley Online Library on [09/01/2024]. See the Terms and Conditions (https://onlinelibrary.wiley.com/terms-and-conditions) on Wiley Online Library for rules of use; OA articles are governed by the applicable Creative Commons License

simple test where 10Fe-$CSiO_x$ is used as electrode in a lithium-ion battery is also performed. Since no additional carbon is needed to increase the conductivity, the electrode preparation process can be significantly simplified. As the active species is currently not known, herein the specific capacity is calculated based on the weight of the material. Figure S28 shows the first 11th electrochemical cycles, where the first discharge capacity is 1684 $mA \cdot h \cdot g^{-1}$ while the first charge capacity is 448 $mA \cdot h \cdot g^{-1}$. Thus, the first Coulombic efficiency is low, and the irreversible capacity is large, likely due to the solid-state electrolyte interface formation and the irreversible structure change of 10Fe-$CSiO_x$. The capacity is gradually stabilized around 300 $mA \cdot h \cdot g^{-1}$ within 10 cycles, indicating 10Fe-$CSiO_x$ could show a good cycling performance. Thus, 10Fe-$CSiO_x$ might be useful as an anode material for lithium-ion batteries. Further optimization is in progress to improve its electrochemical performance.

Conclusions

We developed a quite simple one-pot and one-step method to get a new material family of carbosilicate, in which transition metal ions act as bridging agent for the silicate and carbon structures. The abundant oxygen functional groups of both carbon and silicate in combination form a stable C-O-Fe-O-Si link of the carbosilicate with a homogeneous distribution of the involved elements. The synthesis is also scalable and economically effective with various carbons (can be from waste organic or biomass), silica (can be waste glass) and metals (we only tried Fe, Co, and Ni). The composites display some quite interesting properties, including high surface area, uniform mesoporosity and excellent conductivity. As it is quite adjustable, carbosilicates could also be very useful in many other applications. The areas where carbosilicates can play important roles are under further investigations. The hybridization process may also inspire the reformation and composition of carbon with the commonly used inorganic oxides like TiO_2 or Al_2O_3.

Supporting Information

All the related information can be found in the Supporting information document.

Acknowledgements

The authors thank the Lanzhou Institute of Chemical Physics, Max Planck Society, Chinese Academy of Science and Jilin University for fundings. The authors thank Dr. Yunxiang Qiao for the synthesis of the materials. The authors thank Prof. Robert Schlögl and Prof. Josef Granwehr for the support and the useful discussions. The numerical calculations in this paper have been done on Hefei advanced computing center.

Keywords: Carbosilicate • Graphene nanoribbon • Silicate • ultrathin 2D material • nanocarbon

References

[1] R. Xu, W. Pang, Y. Xu, Q. Huo, *Modern Inorganic Synthetic Chemistry*, Elsevier, **2011**.

[2] E. Fitzer, L. M. Manocha, *Carbon reinforcements and carbon/carbon composites*, Springer Science & Business Media, **1998**.

[3] a) R. Mas-Balleste, C. Gomez-Navarro, J. Gomez-Herrero, F. Zamora, *Nanoscale* **2011**, *3*, 20-30; b) A. K. Geim, K. S. Novoselov, *Nat. Mater.* **2007**, *6*, 183-191; c) K. S. Novoselov, A. K. Geim, S. V. Morozov, D.-e. Jiang, Y. Zhang, S. V. Dubonos, I. V. Grigorieva, A. A. Firsov, *Science* **2004**, *306*, 666-669.

[4] a) M. Alexandre, P. Dubois, *Mater. Sci. Eng. R Rep.* **2000**, *28*, 1-63; b) D. K. James, J. M. Tour, *Acc. Chem. Res.* **2013**, *46*, 2307-2318; c) S. Kim, S. H. Ku, S. Y. Lim, J. H. Kim, C. B. Park, *Adv. Mater.* **2011**, *23*, 2009-2014.

[5] M. Terrones, *Nature* **2009**, *458*, 845-846.

[6] a) L. Jiao, L. Zhang, X. Wang, G. Diankov, H. Dai, *Nature* **2009**, *458*, 877-880; b) D. V. Kosynkin, A. L. Higginbotham, A. Sinitskii, J. R. Lomeda, A. Dimiev, B. K. Price, J. M. Tour, *Nature* **2009**, *458*, 872-876.

[7] L. Wang, D. W. Bahnemann, L. Bian, G. H. Dong, J. Zhao, C. Y. Wang, *Angew. Chem. Int. Ed.* **2019**, *58*, 8103-8108.

[8] a) M. F. Brigatti, D. Malferrari, A. Laurora, C. Elmi, *Structure and mineralogy of layer silicates: recent perspectives and new trends*, **2011**; b) E. P. Giannelis, *Adv. Mater.* **1996**, *8*, 29-35.

[9] a) J. Lim, U. N. Maiti, N. Y. Kim, R. Narayan, W. J. Lee, D. S. Choi, Y. Oh, J. M. Lee, G. Y. Lee, S. H. Kang, H. Kim, Y. H. Kim, S. O. Kim, *Nat. Commun.* **2016**, *7*, 10364; b) J. L. Wang, L. Ma, Q. H. Yuan, L. Y. Zhu, F. Ding, *Angew. Chem. Int. Ed.* **2011**, *50*, 8041-8045.

[10] R. Wlodarczyk, J. Sauer, X. Yu, J. A. Boscoboinik, B. Yang, S. Shaikhutdinov, H. J. Freund, *J. Am. Chem. Soc.* **2013**, *135*, 19222-19228.

[11] a) P. Düngen, R. Schlögl, S. Heumann, *Carbon* **2018**, *130*, 614-622; b) Y. Ding, Z. A. Qiao, *Adv. Mater.* **2022**, *34*, 2206025.

[12] a) D. R. Katti, K. B. Thapa, K. S. Katti, *J. Rock Mech. Geotech. Eng.* **2018**, *10*, 1133-1144; b) D. R. Katti, H. B. Upadhyay, K. S. Katti, *Fuel* **2014**, *130*, 34-45.

[13] Y. Qiao, N. Theyssen, B. Spliethoff, J. Folke, C. Weidenthaler, W. Schmidt, G. Prieto, C. Ochoa-Hernandez, E. Bill, S. Ye, H. Ruland, F. Schuth, W. Leitner, *Dalton Trans.* **2021**, *50*, 850-857.

[14] R. Schlögl, *Adv. Catal*, **2013,** *56, 103-185*.

[15] Y. Ding, Q. Gu, A. Klyushin, X. Huang, S. H. Choudhury, I. Spanos, F. Song, R. Mom, P. Düngen, A. K. Mechler, R. Schlögl, S. Heumann, *J. Energy Chem.* **2020**, *47*, 155-159.

[16] F. Liebau, *Structural chemistry of silicates: structure, bonding, and classification*, Springer Berlin, **1985**.

This article is protected by copyright. All rights reserved.

15213773, ja, Downloaded from https://onlinelibrary.wiley.com/doi/10.1002/anie.202318043 by Fritz-Haber-Institut Der Max-Planck-Gesellschaft, Wiley Online Library on [09/01/2024]. See the Terms and Conditions (https://onlinelibrary.wiley.com/terms-and-conditions) on Wiley Online Library for rules of use; OA articles are governed by the applicable Creative Commons License

10.1002/anie.202318043

[17] S. Brunauer, P. H. Emmett, E. Teller, *J. Am. Chem. Soc.* **1938**, *60*, 309-319.
[18] E. P. Barrett, L. G. Joyner, P. P. Halenda, *J. Am. Chem. Soc.* **1951**, *73*, 373-380.
[19] a) C. Fang, J. Zhou, L. Zhang, W. Wan, Y. Ding, X. Sun, *Nat. Commun.* **2023**, *14*, 4449; b) Y. Ding, M. Greiner, R. Schlögl, S. Heumann, *ChemSusChem* **2020**, *13*, 4064-4068.

This article is protected by copyright. All rights reserved.

15213773, ja, Downloaded from https://onlinelibrary.wiley.com/doi/10.1002/anie.202318043 by Fritz-Haber-Institut Der Max-Planck-Gesellschaft, Wiley Online Library on [09/01/2024]. See the Terms and Conditions (https://onlinelibrary.wiley.com/terms-and-conditions) on Wiley Online Library for rules of use; OA articles are governed by the applicable Creative Commons License

Accepted Manuscript

10.1002/anie.202318043

WILEY VCH

RESEARCH ARTICLE

Entry for the Table of Contents

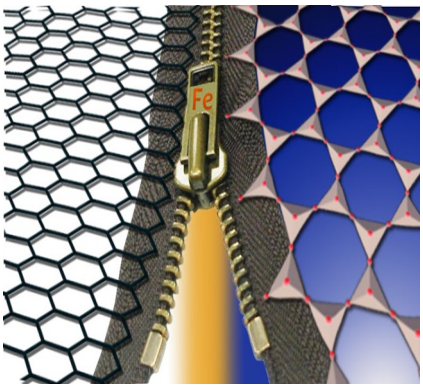

Via unzipping and zipping processes, an ultrathin two-dimensional layered carbosilicate is obtained by hydrothermal treatment. In a one-pot reaction, CNT and bulk silica are unzipped by the reaction of iron and water, followed by iron zipping the unzipped species to form the carbosilicate. The unprecedent phenomenon brings us new insight on synergistic chemistry, stimulating the discovery of new structures and materials.

This article is protected by copyright. All rights reserved.

15213773, ja, Downloaded from https://onlinelibrary.wiley.com/doi/10.1002/anie.202318043 by Fritz-Haber-Institut Der Max-Planck-Gesellschaft, Wiley Online Library on [09/01/2024]. See the Terms and Conditions (https://onlinelibrary.wiley.com/terms-and-conditions) on Wiley Online Library for rules of use; OA articles are governed by the applicable Creative Commons License